



ELSEVIER

Contents lists available at ScienceDirect

Global and Planetary Change

journal homepage: www.elsevier.com/locate/gloplacha

Research paper

Control of seasonal and inter-annual rainfall distribution on the Strontium-Neodymium isotopic compositions of suspended particulate matter and implications for tracing ENSO events in the Pacific coast (Tumbes basin, Peru)

Jean-Sébastien Moquet^{a,b,c,*}, Sergio Morera^{a,d}, Bruno Turcq^e, Franck Poitrasson^b, Martin Roddaz^b, Patricia Moreira-Turcq^{b,d}, Jhan Carlo Espinoza^{a,f}, Jean-Loup Guyot^b, Ken Takahashi^g, Jhon Orrillo-Vigo^a, Susana Petrick^h, Stéphanie Mounic^b, Francis Sondag^b

^a Instituto Geofísico del Perú, Calle Badajoz # 169, Mayorazgo IV Etapa, Ate Vitarte, Lima, Peru

^b Géosciences Environnement Toulouse (GET), UMR 5563 (GET/OMP), CNRS, IRD, Université Paul Sabatier, 14 avenue Edouard Belin, 31400 Toulouse, France

^c Institut de Physique du Globe de Paris (IPGP), Centre National de la Recherche Scientifique, Sorbonne Paris Cité, 1 Rue Jussieu, 75005 Paris, France

^d Universidad Agraria de La Molina, Av. La Molina s/n La Molina, Lima, Peru

^e LOCEAN, IRD/SU/CNRS/MNHN, Centre IRD d'Ile de France, 32 av. Henri Varagnat, 93143 Bondy, Cedex, France

^f Univ. Grenoble Alpes, IRD, CNRS, Grenoble INP, IGE, 3800 Grenoble, France

^g Servicio Nacional de Meteorología e Hidrología del Perú, Jr. Cahuide 785, Jesús María, Lima, Peru

^h Instituto Peruano de Energía Nuclear, Av. Canadá #1470, Lima, Peru

ARTICLE INFO

Keywords:

River
Andes
Pacific basin
Sr and Nd radiogenic isotopes
Suspended sediments
Hydrology

ABSTRACT

The geochemistry of riverine sediments exported to the oceans is important for paleo-hydro-climatic reconstruction. However, climate reconstruction requires a good understanding of the relationship between geochemistry and hydrological variability and sediment sources. In this study, we analyzed the major elements, the strontium-neodymium radiogenic isotopes signatures ($^{87}\text{Sr}/^{86}\text{Sr}$ and ϵNd) and the mineralogy of the suspended particulate matter (SPM) sampled monthly during two hydrologic years (2007–2008, a wet year, and 2010–2011, a normal hydrological year) upstream the Tumbes River outlet. The hydroclimate of this Ecuador-Peru binational basin is particularly sensitive to ENSO (El Niño Southern Oscillation) events.

While mineralogy (dominated by illite) and the chemical alteration index (from 75 to 82) remain almost constant along the two hydrological years, $^{87}\text{Sr}/^{86}\text{Sr}$ (0.7115 to 0.7176) and ϵNd (-7.8 to -1.9) signatures are particularly sensitive to discharge and SPM concentration variations. Along the hydrological year, two sources control the ϵNd variability: (1) volcanic rocks, which dominate during the dry season, and (2) plutonic/metamorphic sources, whose contribution increases during the wet season. This behavior is confirmed by the correlation between ϵNd signature and the monthly rainfall contribution from volcanic area ($R = 0.58$; p -value < 0.01), and also with the daily discharge at the outlet ($R = -0.73$; p -value < 0.01). For most of the samples, $^{87}\text{Sr}/^{86}\text{Sr}$ is less variable along the hydrological year. However, two exceptional high discharge and SPM concentration conditions sampled exhibit more radiogenic (higher) $^{87}\text{Sr}/^{86}\text{Sr}$ signatures when plutonic/metamorphic rocks derived sediments are released in sufficient quantities to notably change the SPM isotopic Sr value of the Tumbes River.

Hence, this study demonstrates that $^{87}\text{Sr}/^{86}\text{Sr}$ and ϵNd signatures can be used as powerful proxies for paleoclimate reconstructions based on sediment core's analysis in relation with spatial rainfall distribution and intensity in Pacific sedimentary basins submitted to the diversity of ENSO events.

1. Introduction

The hydrological and hydro-sedimentological regime of the Andes

are particularly sensitive to extreme hydrological events like those related to the El Niño Southern Oscillation (ENSO) system. The El Niño and its counterpart, La Niña (the two expressions of the ENSO) are

* Corresponding author at: Institut de Physique du Globe de Paris (IPGP), Centre National de la Recherche Scientifique, Sorbonne Paris Cité, 1 Rue Jussieu, 75005 Paris, France.

E-mail address: jean-sebastien.moquet@cnrs-orleans.fr (J.-S. Moquet).

<https://doi.org/10.1016/j.gloplacha.2019.103080>

Received 19 July 2019; Received in revised form 8 November 2019; Accepted 9 November 2019

Available online 12 November 2019

0921-8181/ © 2019 Elsevier B.V. All rights reserved.

drivers of the strongest year-to-year climate fluctuations on the planet. They control the hydrology and sediment production in Andean basins residing both along the Pacific coast (Sulca et al., 2018; Rau et al., 2017; Lavado and Espinoza, 2014, Armijos et al., 2013) and in Amazonian slopes (Espinoza et al., 2012). These events have been responsible for extreme flooding in Pacific coastal areas (particularly in Northern Peru and in Ecuador) and droughts in the Andes and in the Amazon region (Lavado and Espinoza, 2014; Sulca et al., 2018; Espinoza et al., 2012). Importantly, the two main El Niño events of the last 40 years account for around 45% of the sedimentary flux exported to northern Peru Pacific Ocean (Morera et al., 2017). However, ENSO events present a large diversity associated with their tropical Pacific Sea Surface Temperature (SST) anomaly patterns (e.g. Capotondi et al., 2015) and the variability of these patterns can affect even the sign (positive or negative) of the precipitation anomalies in northern Peru (Lavado and Espinoza, 2014; Sulca et al., 2018). Thus, predicting the impact of extreme hydrological events associated with ENSO remains difficult because of the relatively short time-scale of hydrological and riverine suspended matter export monitoring.

The reconstruction of paleo-ENSO events is necessary to understand the main forcing on these events from the Pliocene (e.g. Wara et al., 2005) to Quaternary timescale, including the Holocene (e.g. Carré et al., 2012). Paleo ENSO events have been identified in onshore/continental geological record based on oxygen stable isotope compositions of speleothems (e.g. Bustamante Rosell et al., 2016), authigenic calcite lake sediment cores (Bird et al., 2011) and ice cores from the Ecuadorian and Peruvian Andes (e.g. Thompson et al., 2013). In all of these studies, most of the geochemical tracers used to reconstruct paleo ENSO events in the geological record were aimed at the identification of temperature (oceanic cores) or precipitation (lake cores, speleothems, ice cores) anomalies based on stable isotope geochemistry. To date, there has been little attempts to reconstruct paleo ENSO events based on the identification of peak sediment fluxes linked to rainfall increase in the Andean coast, which can be reflected in the sedimentary record by changes in the provenance of the associated sediments. For instance, change in provenance based on Nd isotopic composition of the detrital sediment fraction during the past 45,000 years have been used to reconstruct climate-driven changes in the provenance of clays deposited

along the Mozambique Margin (van der Lubbe et al., 2016). Similarly, changes in the provenance of sediments deposited along the tropical South American continental margin between Andes and shield regions, identified based on Nd–Sr isotopic composition variations, were also used for reconstructing both erosional and associated rainfall patterns on continental source regions during the Quaternary (e.g. Höppner et al., 2018). Even more recently, variation of Nd isotopic composition of Amazon River suspended particulate material (hereafter designated as “SPM”) during a one year hydrological cycle has been related to seasonal changes in the rainfall distribution patterns across the Amazon basin that are associated with latitudinal migrations of the Intertropical Convergence Zone (Rousseau et al., 2019). The relationship between long-term (Holocene) climate change and changing hydrology and sediment sources using Sr and Nd has been studied in the Nile basin (Woodward et al., 2015). This work illustrates the benefits of using Sr and Nd isotopes in tandem to tease out changes in catchment runoff and sediment delivery. However we have only identified 3 studies exploring Sr and Nd isotopes modern SPM variability along a hydrological year (Viers et al., 2008; Mao et al., 2011; Rousseau et al., 2019). These studies reported significant variability of the Sr and Nd signatures along the hydrological year. While εNd appears to mainly trace the lithological composition of the SPM source, ⁸⁷Sr/⁸⁶Sr can track both the SPM source (Mao et al., 2011) and grain size sorting effects due to either erosional processes (Viers et al., 2008) or hydrodynamical sorting behavior (Rousseau et al., 2019).

In this scenario, the combined use of Sr and Nd isotopes in sedimentary rock as potential tracers of paleo ENSO event may be particularly useful providing that isotopically contrasted rocks are differentially eroded during ENSO and normal years. To explore this possibility, we present the geochemistry and Nd and Sr isotopes composition of the SPM exported by the Tumbes River along contrasted hydrological periods at both the seasonal (dry vs wet season) and inter-annual (wet vs normal years) time scale. For this purpose, we have analyzed monthly sampled SPM at the lower reach of the basin along two hydrological cycles and interpreted the corresponding data as function of discharge, SPM concentration, SPM fluxes, seasonal and inter-annual rainfall distribution and geochemical characteristic of the SPM sources.

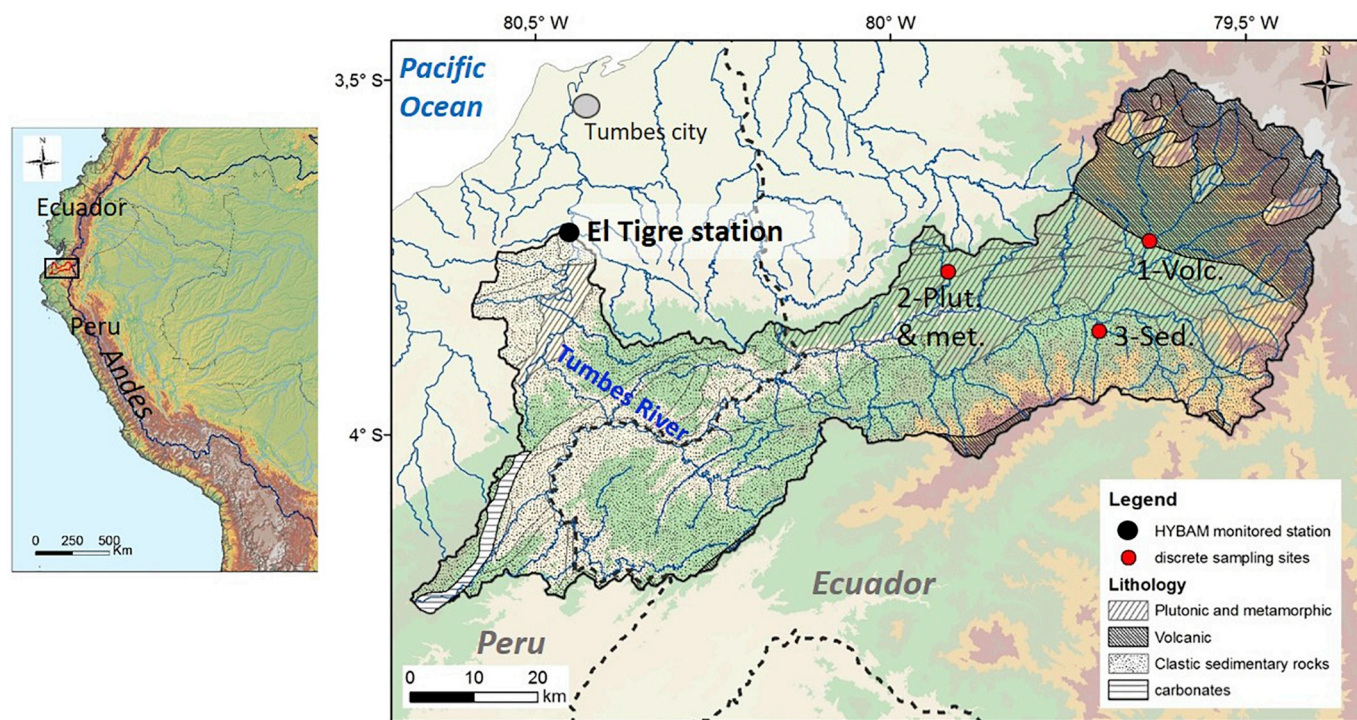


Fig. 1. Map of the Tumbes River basin: hydrological network, lithological domains, national boundaries and sampled stations (1 - Rio Calera @Portovelo – Volcanic area; 2 - Rio Marcabelli @ Marcabelli - Plutonic and metamorphic area and 3 - a rio Pindo tributary @Buenavista – a sedimentary sub-basin).

1.1. Regional setting

The Tumbes River basin is located in Southern Ecuador and Northern Peru (latitude -79.35 and -80.70 decimal degrees). It drains the western slope of the Andes (between longitude -3.47 and -4.25 decimal degree) over an area of $4.8 \cdot 10^3 \text{ km}^2$ including $\sim 70\%$ in the Andean mountains above 500 m.a.s.l. (meter above sea level; Moquet et al., 2018). It originates in the Andes (~ 3800 m.a.s.l.) and flows through a narrow coastal plain until its outlet to the Pacific Ocean. The river drains three main lithologically-contrasted domains: a volcanic, a plutonic/metamorphic and a sedimentary domain representing respectively 17, 25 and 58% of the area (Fig. 1; table S1). The Upper Tumbes basin drains the volcanic domain which consists in Cenozoic and Mesozoic volcanic rocks (elevation = 2014 ± 667 m.a.s.l.; average $\pm 1\text{sd}$). They are composed of andesites, basalts, and locally derived pyroclastic rocks. The mid-altitude Tumbes basin drains the Paleozoic plutonic and metamorphic domain (elevation = 1036 ± 371 m.a.s.l.), which is mainly composed of schists, gabbro, granite and intermediate intrusive rocks (Fig. 1). The remaining part of the basin (elevation = 735 ± 333 m.a.s.l.) is formed by Cenozoic-Mesozoic mudstones, shales, and sandstones as well as locally derived modern alluvial fan deposits and limestones (Fig. 1).

The basin receives a rain amount of around $1000 \text{ mm}\cdot\text{yr}^{-1}$ which leads to a runoff of around $750 \text{ mm}\cdot\text{yr}^{-1}$ (Lavado et al., 2016; Lavado Casimiro et al., 2012). The cumulative annual rainfall tends to increase with elevation. The rainfall regime, and consequently the discharge regime, shows a strong seasonality both in term of quantity and geographical distribution. The rainfall period occurs during austral summer/

fall between December and May (Segura et al., 2019), peaking between February and April in relation to the southernmost position of the Inter-tropical Convergence Zone (ITCZ) (Huaman and Takahashi, 2016; Fig. 2). The rainfall period contributes to around 85% of the annual discharge at El Tigre station (1985–2015 period; using data from SENAMHI - Servicio Nacional de Meteorología e Hidrología -, PEBPT - Proyecto Especial Binacional Puyango Tumbes - and HYBAM - Contrôle géodynamique, hydrologique et biogéochimique de l'érosion/altération et des transferts de matières dans les bassins de l'Amazone, du Congo et de l'Orénoque). The relative contribution of the rainfall amount varies also along the year. While the plutonic/metamorphic domain contribution is almost constant along the year ($\sim 30\%$), the volcanic domain contributes more than $\sim 35\%$ along the September–October–November period and decreases to $\sim 20\%$ during the rest of the year. Therefore, the sedimentary area contributes between $\sim 35\%$ and $\sim 50\%$ of the total amount of rainfall received by the basin during the dry and wet seasons, respectively (Fig. 2).

The main anthropogenic activity is urbanization throughout the city of Tumbes located close to the outlet of the basin, downstream the El Tigre hydrological station (Fig. 1). Small-scale gold mining activity has also been reported upstream in the Puyango and Portovelo-Zaruma sub-basins (Marshall et al., 2018). But, overall, the anthropogenic influence is rather small on sediment production at the Tumbes basin scale.

2. Material and methods

2.1. Studied sites

We analyzed the geochemistry and the mineralogy of the SPM

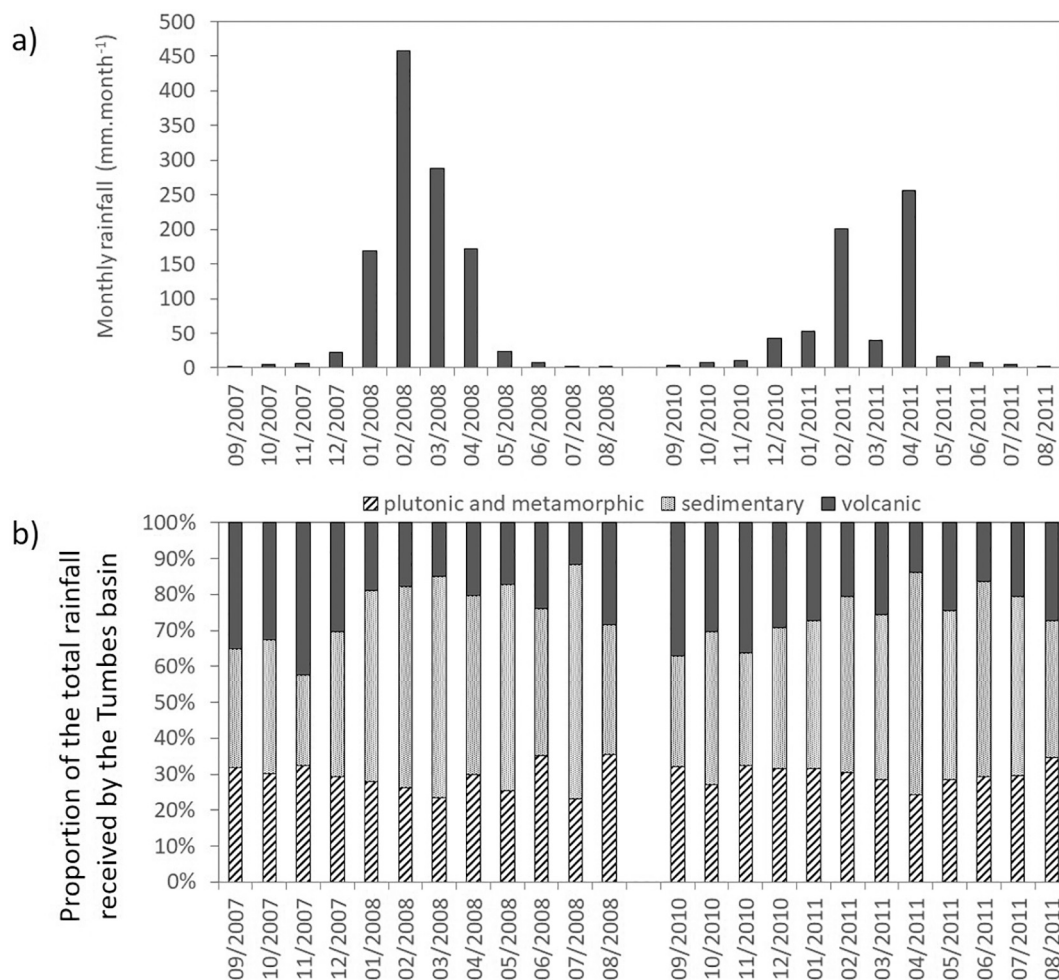


Fig. 2. a) monthly rainfall received by the Tumbes basin b) monthly relative contribution of the rainfall received by the 3 lithological areas (defined on Fig. 1) in the Tumbes Basin along the selected hydrological years (2007–2008 and 2010–2011). Source: monthly rainfall extracted from PISCOv1.1 database (Peruvian Interpolated data of the SENAMHI's Climatological and Hydrological Observations; Lavado et al., 2016).

sampled monthly during two contrasted hydrologic years (2007–2008, a wet year, and 2010–2011, a normal hydrological year) at the El Tigre hydrological station located near the Tumbes River outlet (Fig. 1). We compared these data with the daily discharge and the SPM concentration monitored at this station and with the monthly rainfall data recorded over the basin (see next sections for details). To identify potential source effects which can influence the geochemical and mineralogical composition of the sediments sampled at the El Tigre station, we also performed a discrete sampling of the riverine suspended matter of two Tumbes River tributaries representative of two lithological environments: volcanic and plutonic/metamorphic areas. The Rio Calera at Portovelo drains the volcanic domain and was sampled during 2016 wet season (high water level). The Rio Marcabelli at Marcabelli village drains the plutonic/metamorphic domain and was sampled during 2015 dry season (low water level) and 2016 wet season (high water level). A sedimentary sub-basin (rio Pindo tributary at Buenavista) located downstream a volcanic area and upstream the plutonic/metamorphic area has also been sampled twice (2015 dry season and 2016 wet season) (Table 1, Table S1; Fig. 1). Note that we do not consider this basin as representative of the whole sedimentary area of the Tumbes basin because the sedimentary area located downstream the plutonic/metamorphic area is expected to result on a mix from plutonic/metamorphic and volcanic domains.

2.2. Hydrological and climate data

The hydrological year was considered to be from September to August (Lavado et al., 2016). Mean monthly rainfall was extracted from the PISCOv1.1 Database (Peruvian Interpolated data of the SENAMHI's Climatological and Hydrological Observations; Lavado et al., 2016) for the 1985–2015 period. This gridded rainfall dataset is available at a

monthly frequency for Peru and the regions close to the frontiers with a ~5 km resolution since January 1981. It results from the merging of two rainfall databases: (i) the national rain gauge dataset from the SENAMHI and (ii) the remote sensing rainfall estimates of the Climate Hazards Group Infrared Precipitation (CHIRP; see details in Lavado et al., 2016). This data is freely available from the SENAMHI website (<http://ons.snirh.gob.pe/SOURCES/.Peru/.SENAHMI/.PISCO/.Precipitation/.Monthly/.Precipitation/index.html?Set-Language=fr>). We extracted the monthly rainfall received by the whole basin and by each of the 3 lithological domains (Fig. 2) according to the delimitations defined in Fig. 1.

At the El Tigre SENAMHI/HYBAM station, daily river discharge was available for the 1963–2016 period. In the present study, we considered the 1985–2015 period as the reference. Water levels were measured every 4 h using a conventional hydrological method (Morera et al., 2017). Gauging was accomplished monthly using a mechanical current meter. The daily discharge record was then calculated from rating curves (discharge - water level relationship) using the Hydraccess software (Vauchel, 2005). The daily discharge data are freely available from the HYBAM website (<http://www.so-hybam.org>) until July 2009. The remaining discharge data was provided by the SENAMHI and the PEBPT (<http://pebpt.gob.pe>).

2.3. Suspended particulate matter measurements (SPM)

For SPM concentration measurements, a 650 ml bottle of surface water (10–15 cm from the surface) was sampled each 10 days between 04/02/2004 and 21/04/2014 (387 samples). Only filters of 2006–2011 period were available for geochemical analyses. The sample was filtered through a pre-weighed filter of a 0.45 µm pore size cellulose filter. The filter was dried at 80 °C and weighted to determine the riverine

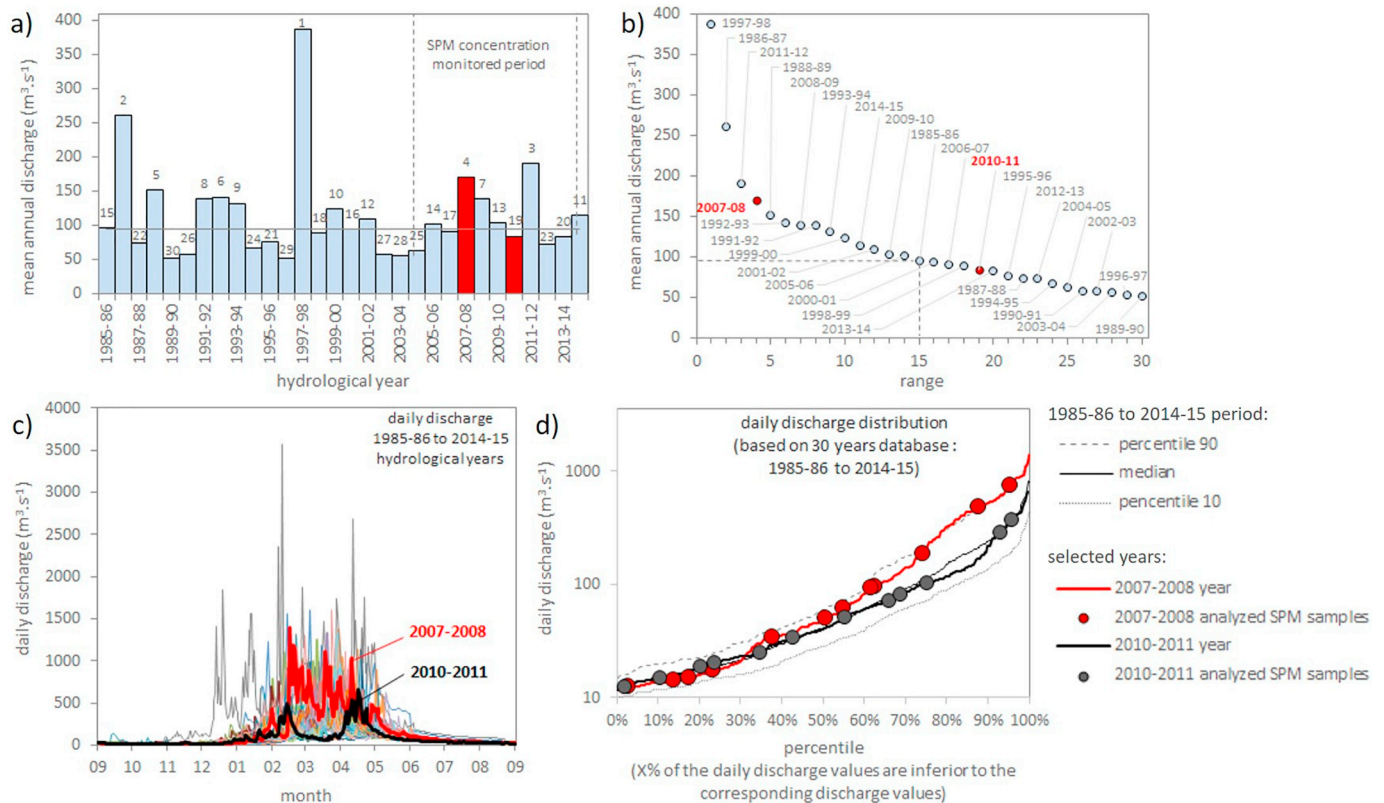


Fig. 3. Hydrological characteristics of the selected years along the 1985–1986 to 2014–2015 period (30 years). a) Annual discharge along the 1985–2015 period. Red bars correspond to the selected years. The median value (95 m³.s⁻¹) is added for reference. The numbers correspond to the range among the 30 years period reference. b) Range of the annual discharge from the wettest to the driest year. Red points correspond to the selected years. c) Hydrogram of the 30 years. d) Distribution of the daily discharge for the 90th, 50th and 10th percentiles (from the lowest to the highest values). The daily discharge distribution of the 2007–2008 and 2010–2011 hydrological years are also reported. The daily discharge for the analyzed SPM samples are reported (see the suppl mat for calculation details). (For interpretation of the references to colour in this figure legend, the reader is referred to the web version of this article.)

SPM concentration.

2.4. Annual flux calculation of monitored rivers

Annual SPM fluxes were calculated based on the 10 days frequency of SPM concentration determinations and daily discharge records. The discharge values of the sampled days are representative of the hydrological conditions of each year recorded at the El Tigre station. We calculated the SPM flux of each sampled day according to the following formula:

$$F_d = C_d \times Q_d \quad (1)$$

with F_d , C_d and Q_d being the daily flux ($t \cdot day^{-1}$), concentration ($mg \cdot l^{-1}$) and discharge ($m^3 \cdot day^{-1}$) of the sampled day. Then, we interpolated the daily SPM flux values to estimate the monthly and the annual flux. According to this power law relationship and to Moatar et al. (2013) method, we estimated the bias and imprecision SPM flux related to the monitoring sampling frequency of the present study. We first estimated the proportion of SPM flux which transited by the station during the upper 2% of highest daily flow ($M2\% = 0.5$; non dimensional). Then, the bias and imprecision were estimated from the equation $y = u M2\%^2 + v M2\%$, where $y = e50$ (bias), $e10$ (10th imprecision percentile) or $e90$ (90th imprecision percentile) and 'u' and 'v' constants are parameters of the error curves for given sampling intervals which are extracted from Moatar et al. (2013) tables. Based on this method, we deduced the bias as being of < 6% and the imprecision ranging from -43% to 39% (see Moatar et al., 2013 for calculation method details). The SPM specific flux ($t \cdot km^{-2} \cdot yr^{-1}$) as well as the specific discharge ($mm \cdot yr^{-1}$) were calculated by dividing, respectively, the SPM flux and the discharge by the total area of the basin at the El Tigre station.

2.5. Selection of the studied years

Among the hydrological years for which we had access to sediment filters (2006–2011 period), we selected the wetter year (2007–2008 hydrological year) and a year close to the median discharge (2010–2011 hydrological year) by comparison with the 30 discharge years along the 09/1985–08/2015 period (Fig. 3a, b). In term of annual discharge, with an annual module of $170m^3 \cdot s^{-1}$, the 2007–2008 year ranks as the 4th wetter year of this 30 years period and exhibits, therefore, a return period of 7.8 years (Fig. 3b). The 2007–2008 period featured to La Niña conditions in the central Pacific, i.e. the Oceanic Niño Index (ONI, <http://www.cpc.ncep.noaa.gov/data/indices/oni.ascii.txt>) was less than -0.5 °C between April 2007 and June 2008 and less than -1 °C between October 2007 and March 2008. It also presented localized positive SST anomaly on the coast of Ecuador and Northern Peru between February and April 2008, both of which promoted precipitation in both the coast and the highlands of Southern Ecuador (Bendix et al., 2011). In the Piura river in Northern Peru (around 5°S), this period produced the largest discharge after the extreme large-scale 1997–1998 and 1982–1983 El Niño and the 1925 coastal El Niño events, even more than other El Niño events. It was due to the nonlinearity of the combination of the effects of the warm coastal and cool central Pacific conditions (Takahashi and Martínez, 2017). Conversely, while the 2010–2011 period also featured La Niña conditions in the central Pacific, it did not present warm coastal conditions.

Discharge records of El Tigre station indicate that the 2007–2008 year ($170 m^3 \cdot s^{-1}$) ranks after the El Niño years of 1997–1998 ($387 m^3 \cdot s^{-1}$) and 1986–1987 ($261 m^3 \cdot s^{-1}$) and the La Niña year of 2011–2012 year ($190 m^3 \cdot s^{-1}$) (Fig. 3b). The lowest annual discharge value recorded along this period ($52 m^3 \cdot s^{-1}$) corresponds to the 1989–1990 hydrological year. The 2010–2011 exhibits a module of $84 m^3 \cdot s^{-1}$, close to the 1985–2015 period median value of $95 m^3 \cdot s^{-1}$. Moreover, the distribution of the daily discharge of the 2010–2011 period is similar to the 1985–2015 period median distribution (Fig. 3c, d). Therefore, the 2010–2011 year is considered as a “normal” year in term of discharge distribution (Fig. 3d). The higher daily discharge (half upper daily discharge values) of the 2007–2008 year is close to the

90th percentile distribution of the 1985–2015 period. In other words, during the 1985–2015 period only 10% of the years (3 years) exhibit higher daily discharge than the 2007–2008 year during the wet period (Fig. 3d).

2.6. Mineralogy and geochemistry

2.6.1. Sample treatments

The 29 selected SPM filters were submerged in ultra-pure water and submitted from 3 to 5 sessions of ultrasonic baths of 30 min until all SPM was visually removed from the filter. The filters were then discarded and the SPM was dried. Between 10 and 300 mg of SPM was therefore recovered from each selected filters. The SPM of each sample was divided into two aliquots. A small (2–3 mg) aliquot was used for X-ray diffraction analyses (DRX) and the remaining sediment was digested for major element concentrations and for Nd and Sr isotopic analyses. This second aliquot was first treated with H_2O_2 for 24 h at ambient temperature, then it was digested in $HNO_3 + HF$ for 36 h at 80 °C, and in $HCl + HNO_3$ for 36 h at 120 °C. Strontium and Nd were separated by ion-exchange chromatography using Sr-SPEC, TRU-SPEC and LN-SPEC resins (Eichrom®) according to the Pin et al. (1994) method. Ultrapure and bi-distilled reagents were used for all digestion and separation steps.

2.6.2. Sample analyses

All analyses were performed at the Géosciences-Environnement-Toulouse (GET) Laboratory - Observatoire Midi-Pyrénées (OMP). X-ray diffraction analyses were carried out using a G3000 Inel diffractometer (40 kV, 30 mA) and Ni-filtered $CuK\alpha_{1,2}$ radiation ($\lambda = 1.5406 \text{ \AA}$). Due to limited amounts of material for some samples, we did not perform a glycol treatment for clay mineral identification. We performed a semi-quantitative estimate of the chlorite, illite, kaolinite and smectite abundance based on the Biscaye (1965) method (Table S2).

Major element analyses were measured by ICP-OES (Horiba Jobin Yvon Ultima2). Measurement accuracy was assessed by processing 5 and 10 mg of the GA basalt reference material (CRPG; Centre de Recherches Pétrographiques et Géochimiques). The Chemical Index of Alteration (CIA) is generally used to estimate the degree of weathering of a basin (e.g. Viers et al., 2008; Rousseau et al., 2019). During weathering, alkali metal and alkaline earth ions are released into solution, whereas alumina is preferentially retained in the weathered material and the CIA is calculated as follows:

$$CIA = [Al_2O_3 / (Al_2O_3 + CaO * + Na_2O + K_2O)] \times 100 \text{ (molar proportions)} \quad (2)$$

where CaO^* is the CaO content in the silicate fraction.

The CIA of the GA reference standard is 59 (recommended value; CRPG) whereas we obtained 55 and 61 for the two GA aliquot analyzed in the present study. An error of up to 4 in this CIA molar ratio is therefore considered in our result presentation (Table 1).

Neodymium and Strontium isotope measurements were conducted on a Triton Thermal Ionization Mass Spectrometer. Neodymium isotope ratios were measured in static mode, corrected for instrumental mass bias fractionation using a $^{146}Nd/^{144}Nd$ ratio of 0.7219. One analysis of the La Jolla standard gave a $^{143}Nd/^{144}Nd$ ratio of 0.511858 ± 16.10^{-6} ($\pm 2 \sigma$; internal precision) in agreement with the recommended value of 0.511858 (Lugmair et al., 1983). Repeated analyses of Rennes standard gave a $^{143}Nd/^{144}Nd$ ratio of 0.511947 ± 10.10^{-6} to 0.511969 ± 16.10^{-6} ($N = 3$; $\pm 2 \sigma$; external precision - 1 week) in agreement with the value recommended by Chauvel and Blichert-Toft (2001) for the Rennes Nd standard ($^{143}Nd/^{144}Nd = 0.511961 \pm 13.10^{-6}$; 2σ). Neodymium isotopes are reported using the ϵNd notation, normalizing samples to the CHondritic Uniform Reservoir (CHUR) value of $^{143}Nd/^{144}Nd = 0.512638$ (Jacobsen and Wasserburg, 1980):

$$\epsilon Nd = \left(\frac{(^{143}Nd/^{144}Nd)_{measured}}{(^{143}Nd/^{144}Nd)_{CHUR}} - 1 \right) \times 10^4 \quad (3)$$

Strontium isotope ratios were measured in dynamic mode, corrected

Table 1

Suspended Particulate Matter (SPM) concentration, daily and monthly discharge (Qj and Qmens respectively), Sr and Nd isotope signature ($\pm 2 \sigma$; 95% confidence level) and Chemical Index Alteration (CIA) values of the sampled SPM. The CIA error is up to 4 (see Section 3 for details).

Type sample	Date	Digested sample weight	SPM conc.	Qj	Qmens	$^{87}\text{Sr}/^{86}\text{Sr}$		$^{143}\text{Nd}/^{144}\text{Nd}$		ϵNd		CIA
						Mean	$\pm 2 \sigma$	Mean	$\pm 2 \sigma$	Mean	$\pm 2 \sigma$	
						$\times 10^{-6}$		$\times 10^{-6}$		(error = 4)		
		mg	mg.l ⁻¹	m ³ .s ⁻¹								
Volcanic	28/02/2016 (HW)	256				0.705873	7	0.512622	21	-0.32	0.40	84
Sedimentary	01/10/2015 (LW)	30				0.706347	18	0.512676	4	0.73	0.08	71
	27/02/2016 (HW)	19				0.705780	5	0.512775	7	2.66	0.15	87
Plutonic/ metamorphic	27/02/2016 (LW)	7				0.729165	9	0.512118	2	-10.14	0.05	81
	01/10/2015 (HW)	12				0.729020	8	0.512083	5	-10.82	0.11	81
Rio Tumbes	11/09/2007	6	23	17	18	-	-	0.512541	6	-1.89	0.12	80
Rio Tumbes	11/10/2007	9	29	15	15	0.712726	8	0.512493	10	-2.83	0.19	80
Rio Tumbes	11/11/2007	14	46	14	24	0.712700	9	0.512396	7	-4.72	0.14	82
Rio Tumbes	11/12/2007	11	39	12	74	0.711989	8	0.512420	5	-4.25	0.10	80
Rio Tumbes	11/01/2008	27	83	61	99	0.713399	9	0.512316	15	-6.28	0.30	79
Rio Tumbes	11/02/2008	114	42	95	506	0.712309	10	0.512327	7	-6.06	0.14	77
Rio Tumbes	11/03/2008	181	2665	475	581	0.717629	11	0.512240	5	-7.76	0.10	80
Rio Tumbes	11/04/2008	92	2284	736	446	0.715501	17	-	-	-	-	75
Rio Tumbes	11/05/2008	39	204	186	195	0.713068	8	0.512256	10	-7.46	0.19	78
Rio Tumbes	11/06/2008	11	41	92	84	0.712805	6	0.512338	14	-5.86	0.27	80
Rio Tumbes	11/07/2008	8	28	50	47	0.711790	9	0.512358	15	-5.46	0.29	79
Rio Tumbes	11/08/2008	12	39	34	34	0.712213	8	0.512424	5	-4.17	0.10	81
Rio Tumbes	11/09/2010	27	94	20	20	0.713872	11	0.512412	8	-4.41	0.15	82
Rio Tumbes	11/10/2010	19	91	15	16	0.711846	9	0.512485	8	-2.98	0.15	81
Rio Tumbes	11/11/2010	13	50	12	14	0.711565	9	0.512505	6	-2.59	0.11	81
Rio Tumbes	11/12/2010	30	146	19	25	0.711876	8	0.512294	19	-6.70	0.38	81
Rio Tumbes	11/01/2011	37	167	71	95	0.712520	10	0.512362	12	-5.39	0.24	81
Rio Tumbes	11/02/2011	107	188	288	225	0.712581	6	0.512304	5	-6.52	0.10	77
Rio Tumbes	11/03/2011	16	50	82	91	0.712700	1	0.512364	5	-5.34	0.10	80
Rio Tumbes	11/04/2011	46	731	366	332	0.712518	7	0.512327	6	-6.07	0.12	81
Rio Tumbes	11/05/2011	20	63	102	99	0.711504	8	0.512457	8	-3.52	0.15	80
Rio Tumbes	11/06/2011	21	77	51	48	0.711646	11	0.512430	6	-4.06	0.12	80
Rio Tumbes	11/07/2011	22	93	33	35	0.712390	15	0.512420	4	-4.25	0.08	81
Rio Tumbes	11/08/2011	31	103	25	25	-	-	0.512514	9	-2.42	0.18	80

for instrumental mass bias using $^{88}\text{Sr}/^{86}\text{Sr} = 0.1194$. Repeated analyses of the NBS 987 standard gave a $^{87}\text{Sr}/^{86}\text{Sr}$ ratio of 0.710256 ± 15.10^{-6} (2σ , external precision, $N = 6$ during two weeks) in agreement with the value recommended by Hodell et al., (2007) ($^{87}\text{Sr}/^{86}\text{Sr} = 0.710240 \pm 15.10^{-6}$; 2σ).

2.6.3. Correlation analysis

All correlation analyses presented in the present study are performed along the whole SPM dataset collected at the El Tigre station and analyzed ($N = 21, 22, 23$ or 24 according to the considered data). Only significant correlation at p -value $< .01$ are considered. Therefore, the correlation is significant at p -value $< .01$ when $R > 0.526, 0.515, 0.505$ and 0.496 for $N = 21, 22, 23$ and 24 respectively. The best fit was observed considering relationships between discharge, rainfall, SPM concentration and SPM flux according to logarithm scales and $^{88}\text{Sr}/^{86}\text{Sr}$, ϵNd and the relative rainfall distribution by lithological areas according to linear scales.

3. Results

3.1. Hydro-sediment budgets

During the sampled years, the daily water discharge corresponding to sampling ranged from $12 \text{ m}^3\text{s}^{-1}$ (November 2010) to $736 \text{ m}^3\text{s}^{-1}$ (March 2008) and the SPM concentration varies from 2 to $7350 \text{ mg}\cdot\text{l}^{-1}$. The latter follows broadly a power law relationship with daily discharge for discharges conditions up from around $40 \text{ m}^3\text{s}^{-1}$ (Fig. 4). The SPM concentration remains almost constant for discharge lower than this value (Morera et al., 2017). During the 2007–2008 and the 2010–2011 hydrological years, the Tumbes River exported 1835 and $190 \text{ t}\cdot\text{km}^{-2}\cdot\text{yr}^{-1}$ of sediments at El Tigre station, respectively.

3.2. Mineralogy

The DRX analyses show that the sampled SPM at El Tigre station are dominated by illite ($88 \pm 7\%$ of the clays; ± 1 sd-standard deviation) followed by chlorite ($9 \pm 2\%$) while kaolinite and smectite represent $< 3\%$ of the clays. This clay composition does not vary with the seasonal hydrological variation. The sampled monolithological sub-basins exhibit almost the same mineralogical composition (Fig. S1; Table S2).

According to these DRX analyses, feldspar and gibbsite are not detected in all samples whereas quartz is systematically detected. However, as for clays, no relationship between quartz abundance and discharge is observed. Interestingly, the monolithological volcanic and sedimentary sub-basin samples can exhibit a slightly higher signal of amphibole, feldspath, gibbsite and quartz (Table S2).

3.3. Geochemistry

The CIA of the El Tigre station SPM ranges between 75 and 82. This low variability reflects a relatively homogenous chemical weathering state of the sediments. With values ranging from 71 to 87, the discrete sampling of monolithological volcanic, plutonic/metamorphic and sedimentary basins exhibit the same range of CIA values (Table 1). This spatial CIA homogeneity from upstream to the basin outlet shows that no significant weathering processes affect the exported sediments throughout their transport.

The ϵNd SPM values range from -7.8 to -1.9 and follow a seasonal behavior negatively correlated with discharge and, therefore, the SPM concentration. The minimum ϵNd value is observed during the rainy season (Fig. 5). The $^{87}\text{Sr}/^{86}\text{Sr}$ isotopic composition of analyzed SPM ranges from 0.7115 to 0.7176. The variability of $^{87}\text{Sr}/^{86}\text{Sr}$ is low for most of the samples (0.7115 to 0.7139) with the exception of the March and April 2008 samples which exhibit higher values (0.7176 and

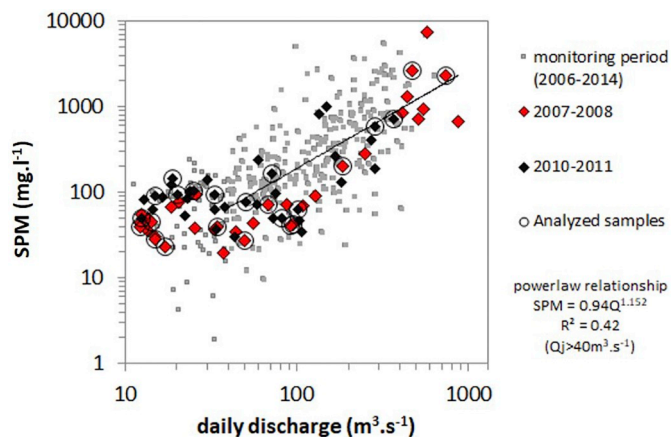


Fig. 4. Suspended Particulate Matter (SPM) concentration as function of daily discharge of the Tumbes R. at El Tigre station along the 2006–2014 period. Data of the 2007–2008 and the 2010–2011 hydrological years are distinguished. The samples analyzed for geochemistry are also identified for reference. The SPM vs daily discharge powerlaw relationship is added for reference for daily discharge upper than 40 m³.s⁻¹.

0.7155 respectively). Interestingly, these two months correspond to the highest SPM concentration recorded for the analyzed samples and correspond to high discharge conditions (Table 1; Fig. 5). The ⁸⁷Sr/⁸⁶Sr and εNd values are significantly negatively correlated ($R = -0.54$; p -value < .01) suggesting a first order opposite behavior.

The volcanic basin SPM sample has Nd and Sr isotope composition of respectively εNd = -0.3 and ⁸⁷Sr/⁸⁶Sr = 0.7059. By contrast the two samples from the plutonic/metamorphic basin exhibits the lower Nd and the higher Sr isotope compositions (εNd = -10.1 and -10.8; ⁸⁷Sr/⁸⁶Sr = 0.7090 and 0.7092). The sampled sedimentary tributary exhibits slightly higher Nd isotope and comparable Sr isotope

compositions relative to the volcanic basin (εNd = 0.7 and 2.7; ⁸⁷Sr/⁸⁶Sr = 0.7058 and 0.7063; Table 1).

Considering both hydrological cycles (Figs. 5, 6), Nd and Sr isotopic compositions are significantly correlated (p -value < .01) with both discharge variability and SPM concentration. In detail, the εNd is better negatively correlated with discharge variability ($R = -0.72$; Fig. 6a) than with SPM concentration ($R = -0.58$; Fig. 6b) while ⁸⁷Sr/⁸⁶Sr is better correlated with SPM concentration ($R = 0.75$; Fig. 6e) than with discharge variability (Fig. 4), both ⁸⁷Sr/⁸⁶Sr and εNd signatures are very well correlated with SPM fluxes ($R = -0.71$ and 0.72 respectively; Fig. 6c and g). However, it is important to highlight that for Sr isotopes significant correlation is controlled by two extreme discharges and SPM concentration values recorded during the wet hydrological cycle (2007–2008; samples of March and April 2008; Table 1).

4. Discussion

4.1. Homogenous mineralogical composition of the Tumbes River

The SPM mineralogy values recorded in the Tumbes river and its monolithological sub-basin tributaries are relatively homogenous (Fig. S1, Table S2). This parameter is therefore not discriminant for tracing the source variability of the riverine suspended sediments. Interestingly, the mineralogical composition of the analyzed samples is enriched in illite and depleted in kaolinite and smectite by comparison with those of the Peruvian and Ecuadorian Andino-Amazonian basins. There, kaolinite, smectite and illite represent around $29 \pm 14\%$ and $40 \pm 20\%$ and $26 \pm 14\%$ (± 1 sd) of the clays (among 30 river bank sediments samples from Napo, Marañon and Ucayali basins; Guyot et al., 2007). As suggested by Liu et al. (2016) to explain clay mineralogical composition diversity in fluvial sediments of South China Sea, physical erosion and chemical weathering regimes can be invoked to explain this Andean Western vs Eastern slope mineralogical contrast.

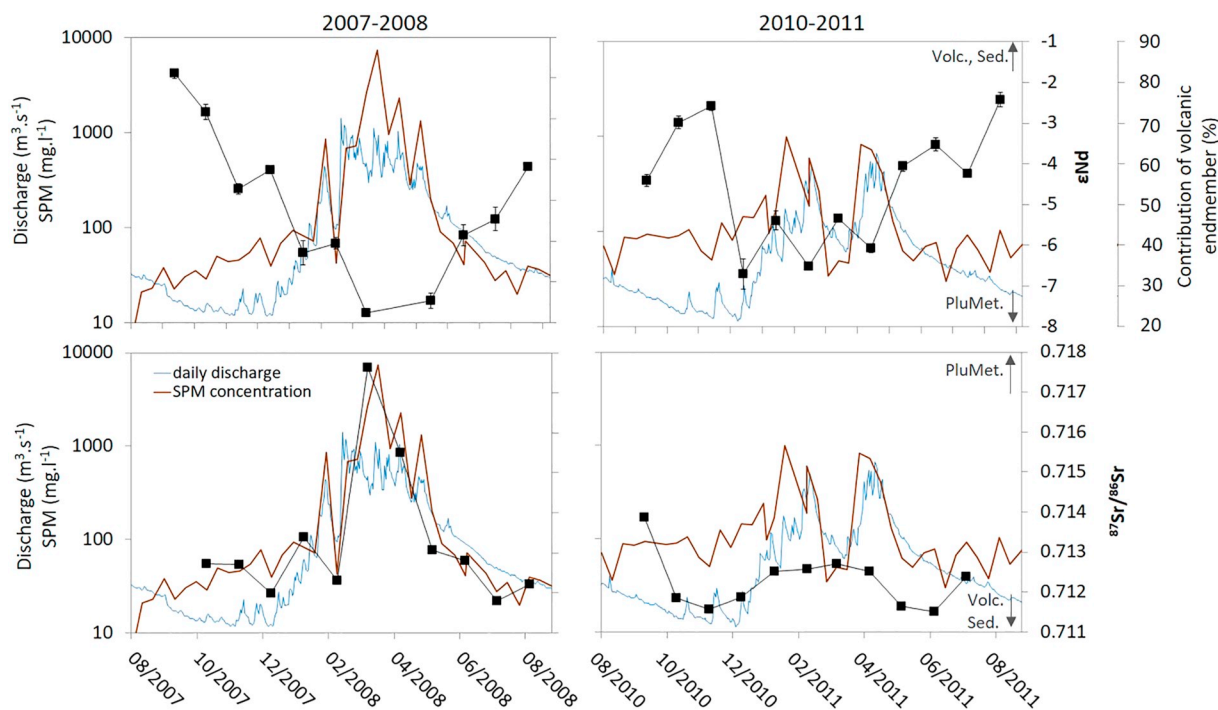


Fig. 5. Variation of daily discharge (blue line), SPM concentration (brown line), εNd and Sr isotopes composition (black line and squares) of the Tumbes River SPM at El Tigre station during the two selected hydrological cycles. The error on ⁸⁷Sr/⁸⁶Sr is smaller than the symbol size. The relative contribution of SPM source calculated from Eq. (4) is added for reference (same symbol as εNd as it results from a proportional relationship). The abbreviation Volc, PluMet and Sed refers to the values determined for SPM samples from the volcanic (εNd = -0.3 and ⁸⁷Sr/⁸⁶Sr = 0.7059), the plutonic/metamorphic (εNd = -10.1 and -10.8; ⁸⁷Sr/⁸⁶Sr = 0.7090 and 0.7092) and the sedimentary (εNd = 0.7 and 2.7; ⁸⁷Sr/⁸⁶Sr = 0.7058 and 0.7063) sub-basins, respectively (see Section 3 for details). (For interpretation of the references to colour in this figure legend, the reader is referred to the web version of this article.)

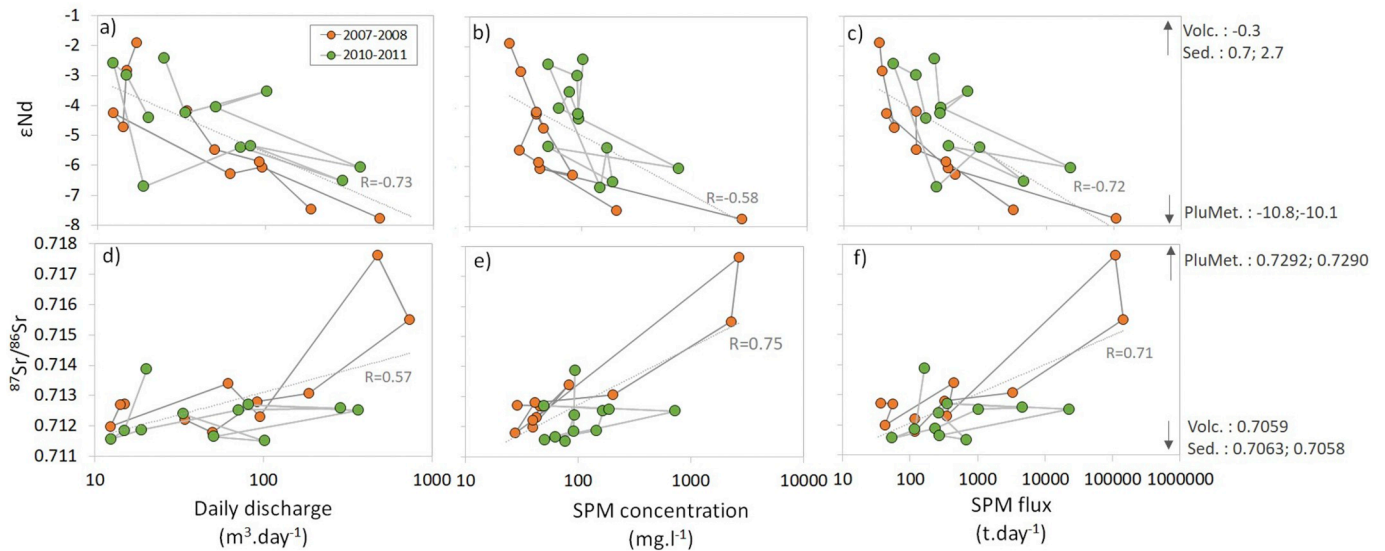


Fig. 6. ϵNd vs a) daily discharge; b) SPM concentration and c) daily SPM flux. $^{87}\text{Sr}/^{86}\text{Sr}$ vs d) daily discharge; e) SPM concentration and f) daily SPM flux. Correlation coefficients consider all points of both hydrological cycles and are all significant (p -value < .01). The abbreviation Volc, PluMet and Sed refers to the values determined for SPM samples from the volcanic, the plutonic/metamorphic and the sedimentary sub-basins, respectively (see Section 3 for details).

Higher illite and chlorite content in the Pacific slope of the Andes can be related to the stronger physical erosion recorded over this area (Armijos et al., 2013; Morera et al., 2017) while high contents of smectite and kaolinite in Amazonian slope can be attributed to the higher weathering intensity measured in the eastern slope of the Andes (Moquet et al., 2011, 2014, 2018).

4.2. Geochemical signature as a proxy of SPM sources

The SPM CIA values recorded in the Tumbes river and its monolithological sub-basin tributaries are quite similar (Table 1). Therefore, the CIA cannot be used for tracing the source of the riverine suspended sediments. The ϵNd and $^{87}\text{Sr}/^{86}\text{Sr}$ isotopic composition of sedimentary rocks or of riverine SPM have been proven to be robust tools for determining their provenance (e.g., McLennan et al., 1993; Allègre et al., 1996; Krom et al., 2002; Goldstein and Hemming, 2003; Faure and Mensing, 2004; Viers et al., 2008; Singh et al., 2008; Roddaz et al., 2014; Höppner et al., 2018; Rousseau et al., 2019) when the sources are isotopically contrasted. However in some cases, these isotopic signatures can be controlled by grain size due to sorting effect (Blum and Erel, 2003; Bouchez et al., 2011; Roddaz et al., 2014; Bayon et al., 2015) especially for Sr isotopes. In the Tumbes River and its tributaries, the mineralogy and the CIA do not vary. Moreover, no significant correlation is observed between mineralogy content, CIA and isotopic signatures. While almost constant mineralogy and CIA values reflect a quite homogenous weathering regime throughout the basin, SPM Nd and Sr isotope signature is mainly controlled by source effect for most of the samples.

The Nd and Sr isotopic composition of Tumbes SPM have intermediate isotopic values between volcanic/sedimentary basins and plutonic/metamorphic basins, suggesting that they correspond to a mixing of these two sources endmembers. Interestingly, sampled SPM from plutonic/metamorphic sub-basins and from volcanic and sedimentary basins are particularly contrasted in term of $^{87}\text{Sr}/^{86}\text{Sr}$ and ϵNd signatures. The volcanic and sedimentary basins SPM exhibit similar Sr–Nd isotopic composition as those of the Jurassic to Quaternary Andean volcanic rocks Andean (Scott et al., 2018; Ancellin et al., 2017) while the SPM from the plutonic and metamorphic area plots on the Subandean domain (Roddaz et al., 2005; Fig. 7). A simple mixing equation between two endmembers (volcanic basin vs plutonic/metamorphic basin) based on Nd isotope ratio allows to estimate the proportion of SPM produced by the volcanic domain (or sediments in the case of the sedimentary basin) according to the following formula:

$$\%SPM_{volc} = \frac{\epsilon\text{Nd}_{sample} - \epsilon\text{Nd}_{plu\ met}}{\epsilon\text{Nd}_{volc} - \epsilon\text{Nd}_{plu\ met}} \quad (4)$$

with $\%SPM_{volc}$ being the relative proportion of the Tumbes SPM derived from the volcanic domain and ϵNd_{volc} , $\epsilon\text{Nd}_{plu\ met}$ and $\epsilon\text{Nd}_{sample}$, representing the ϵNd value of the volcanic basin, plutonic/metamorphic basin and Tumbes SPM respectively.

According to this calculation, around 24 to 74% of the Tumbes SPM are derived from the volcanic endmember and the contribution of the volcanic endmember is negatively correlated with the discharge (Figs. 5 and 6). Indeed, volcanic/sedimentary and plutonic/metamorphic material dominate the SPM production during the dry and wet period respectively. –

4.3. Relationship between Sr–Nd isotopic composition and hydro-climatic variables

4.3.1. Nd isotopic composition

The observed correlations between Nd isotopic composition with SPM concentration and discharge suggest that these isotopic compositions can be considered as good proxies of the seasonal and inter-annual SPM fluxes variability in the Tumbes basin. Indeed, during both analyzed hydrological years, Nd isotopes vary from volcanic to plutonic/metamorphic basin endmembers signature at seasonal timescale (Figs. 5 and 6). During low water level period, SPM Nd isotope signature is closer to the volcanic/sedimentary endmember while the plutonic/metamorphic endmember appears to influence more the SPM geochemistry during high level water season (Fig. 6a). These results suggest that SPM ϵNd values are sensitive to the distribution of rainfall throughout the studied basin. During the low discharge season, maximum rainfall occurs more upstream the basin, in the volcanic and upper sedimentary domains, while during the high water stage, the proportion of rainfall received by the lower part of the basin and the corresponding sediments generated from this area that includes plutonic and metamorphic rocks, are higher (Fig. 2b). This interpretation is confirmed when comparing the daily discharge, monthly discharge and ϵNd values with the monthly relative rainfall distribution throughout the basin (Fig. 8e–g). The rainfall database PISCO is only available at a monthly timescale. However, monthly discharge and rainfall can serve as an appropriate representation of sampled daily discharge based on the observed high correlation value between daily discharge and monthly discharge ($R = 0.91$; Fig. 8i), the monthly discharge and the monthly rainfall ($R = 0.72$; Fig. 8b), and, therefore, between the daily sampled discharge and the monthly rainfall

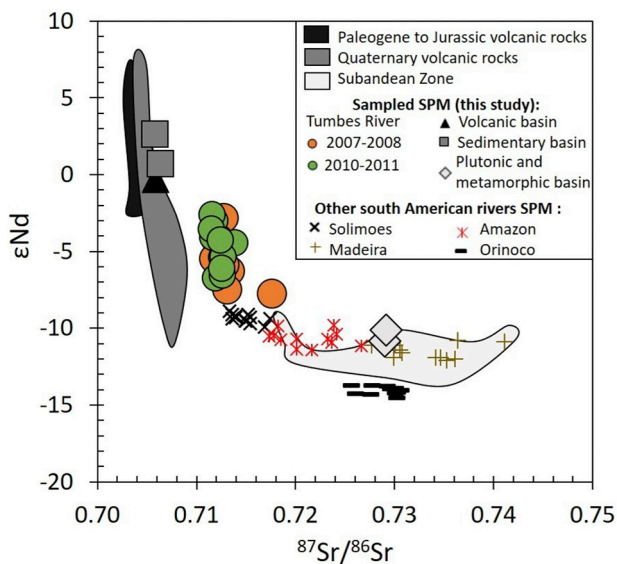


Fig. 7. $^{87}\text{Sr}/^{86}\text{Sr}$ versus ϵNd diagram for Tumbes R. and tributaries sediments (this study). Volcanic rocks domains are extracted from Scott et al. (2018) and Ancellin et al. (2017) and Subandean zone domain was defined by Roddaz et al. (2005). We also reported monthly sampled SPM composition of the Madeira, the Solimoes (Viers et al., 2008), the Amazon and the Orinoco (Rousseau et al., 2019). These values correspond to the modern composition.

($R = 0.68$, Fig. 8a). Thus, the contribution from the volcanic area in terms of mean monthly rainfall was found to be significantly (negatively) correlated to monthly discharge at the outlet ($R = -0.74$; Fig. 8e) and, therefore, to the Nd isotopic composition of SPM sampled at the station ($R = 0.58$; Fig. 8f). These results demonstrate that the Nd isotopic composition of SPM is an excellent proxy of rainfall amount (Fig. 8c) and spatial rainfall distribution (Fig. 8f) of the Tumbes basin which are linked to the outlet discharge.

4.3.2. Sr isotopic composition

Whereas strontium isotopic composition also exhibits significant correlation with the seasonal and inter-annual SPM fluxes variability in the Tumbes basin (Fig. 6f), it is important to highlight that this is essentially due to two extreme discharge and SPM concentration values occurring during the wet hydrological year (2007–2008 year). Otherwise, the $^{87}\text{Sr}/^{86}\text{Sr}$ appears less sensitive than ϵNd to the source variability in the Tumbes Basin.

Such Sr isotopes ratio anomalies have previously been reported for multi-millennial rainfall events based on sediments cores records (e.g. Krom et al., 2002; Höppner et al., 2018) and, in these cases, it was interpreted as a source effect. In the modern SPM Tumbes River, it thus appears that only during extreme hydrological events the high $^{87}\text{Sr}/^{86}\text{Sr}$ typical of plutonic/metamorphic rocks is released in sufficient quantities to notably change the SPM $^{87}\text{Sr}/^{86}\text{Sr}$ value of the Tumbes River. A second possible explanation is that the $^{87}\text{Sr}/^{86}\text{Sr}$ fractionation can be affected by grain size sorting (Bouchez et al., 2011). A third possible explanation is that a larger proportion of the fresher part of these rocks are then eroded under such extreme hydrological events, whereas under normal conditions, radiogenic Sr from these rocks is rather leached through weathering. Suspended particulate matter grain size measurements and concomitant geochemical analysis of the particulate and the dissolved fraction of the same water samples would be required to evaluate these hypotheses.

4.3.3. Suspended particulate matter Sr and Nd isotopic composition in South American rivers

Suspended particulate matter Sr and Nd isotopic composition have also been measured monthly in other South American large rivers. Interestingly, the SPM ϵNd measured at the outlets of the Solimoes, the Madeira (Viers et al., 2008), the Amazon and the Orinoco outlets

(Rousseau et al., 2019) exhibits a low amplitude ranging from 0.8 (Orinoco) to 1.6 (Amazon; the amplitude being defined as the difference between the minimum and the maximum ϵNd value recorded along the year in each river). These values are much lower than the amplitude of 5.9 recorded in the Tumbes River (Table 1; Fig. 7). Conversely these large rivers exhibit an amplitude of $^{87}\text{Sr}/^{86}\text{Sr}$ values ranging from 0.0041 (Solimoes) to 0.0134 (Madeira), thus much higher than the Tumbes river (0.0024), when the two extreme values of the 2007–2008 year are excluded (0.0061 when these two values are included). These differences can be explained, to a first order, by the $^{87}\text{Sr}/^{86}\text{Sr}$ vs ϵNd isotopic mixing curve (Fig. 7). As the Tumbes river SPM is predominantly derived from Andean volcanic lithologies, ϵNd variability is more sensitive to SPM source changes, and therefore to hydrological variability, than $^{87}\text{Sr}/^{86}\text{Sr}$ isotopic signature. Conversely, in the large rivers of the Amazon and Orinoco Basins, the metasedimentary and/or cratonic rocks contribute proportionally more to the SPM composition (Viers et al., 2008; Rousseau et al., 2019). Therefore, changes in SPM source along the hydrological year would affect more the $^{87}\text{Sr}/^{86}\text{Sr}$ SPM signature than the ϵNd . This observation highlights that the initial local lithology has important implications in term of $^{87}\text{Sr}/^{86}\text{Sr}$ and ϵNd SPM sensitivity in response to source and, therefore, to rainfall distribution variability.

To conclude, given the climatic and geological context studied here, variation in Nd and Sr isotopic composition of SPM are, respectively, powerful proxies of the seasonal and inter-annual discharge changes and these properties can be exploited for paleoclimate reconstruction based on sedimentary records.

4.4. Implication for paleo ENSO and paleo extreme hydrologic event reconstruction

Most of paleoclimate reconstruction based on Sr–Nd isotopic composition of marine core sediments are based on a single SPM sampling of the different tributaries or rivers which fed the marine sediments (e.g. Ehlert et al., 2013; Li et al., 2015; Höppner et al., 2018). The dataset presented in this study can be used to improve this approach in Pacific coastal regions affected by ENSO events. Being sensitive to seasonal rainfall distribution (mainly ϵNd) and interannual high rainfall anomalies ($^{87}\text{Sr}/^{86}\text{Sr}$), these isotopic signatures may be particularly useful to reconstruct the paleoclimatology of the studied basin which is highly sensitive to El Niño events (Morera et al., 2017). In addition, the results of this study can be extended beyond the Tumbes River paleoclimate reconstruction and applied to other Peruvian and Ecuadorian Pacific coast basins affected by the ENSO events. For instance, Nd and Sr isotopic variability along Pacific margin sediments cores has previously been interpreted as a function of the upwelling redistributions of the terrigenous sediments produced by rivers, which exhibit contrasted signatures between 0° and 18°S (Ehlert et al., 2013). In the present study, we propose a new and complementary perspective to interpret such records. The altitudinal and spatial rainfall distribution over these basins also needs to be taken into account in order to interpret the geochemistry of these marine core sediments. In fact, in Ecuador and Peru, the Pacific coastal basins are characterized by similar lithological repartitions characterized by volcanic rocks in elevated regions and plutonic and metamorphic rocks in lower elevated regions (Fig. S2). The sedimentary formations would result from their respective upstream erosion processes either mixed, in case of contrasted lithology upstream, or homogenous, when this area drains an homogenous lithological formation as it is the case for the sedimentary sub-basin sampled in the present study. During ENSO events, the rainfall intensity and repartition are modified and can either increase or decrease in both areas even if this effect decreases southward (Lagos et al., 2008; Lavado and Espinoza, 2014). Indeed, according to Lavado and Espinoza (2014), during strong El Niño events and coastal El Niño events, Northern Peruvian Pacific basins are subjected to significant increases in rainfall, while the rainfall decreases in the Southern Peruvian basins (especially in the elevated areas). However, during La Niña events, positive rainfall anomalies are recorded in the upper part of the basins (e.g. Sulca et al., 2018). Based on a regionalization of the rainfall

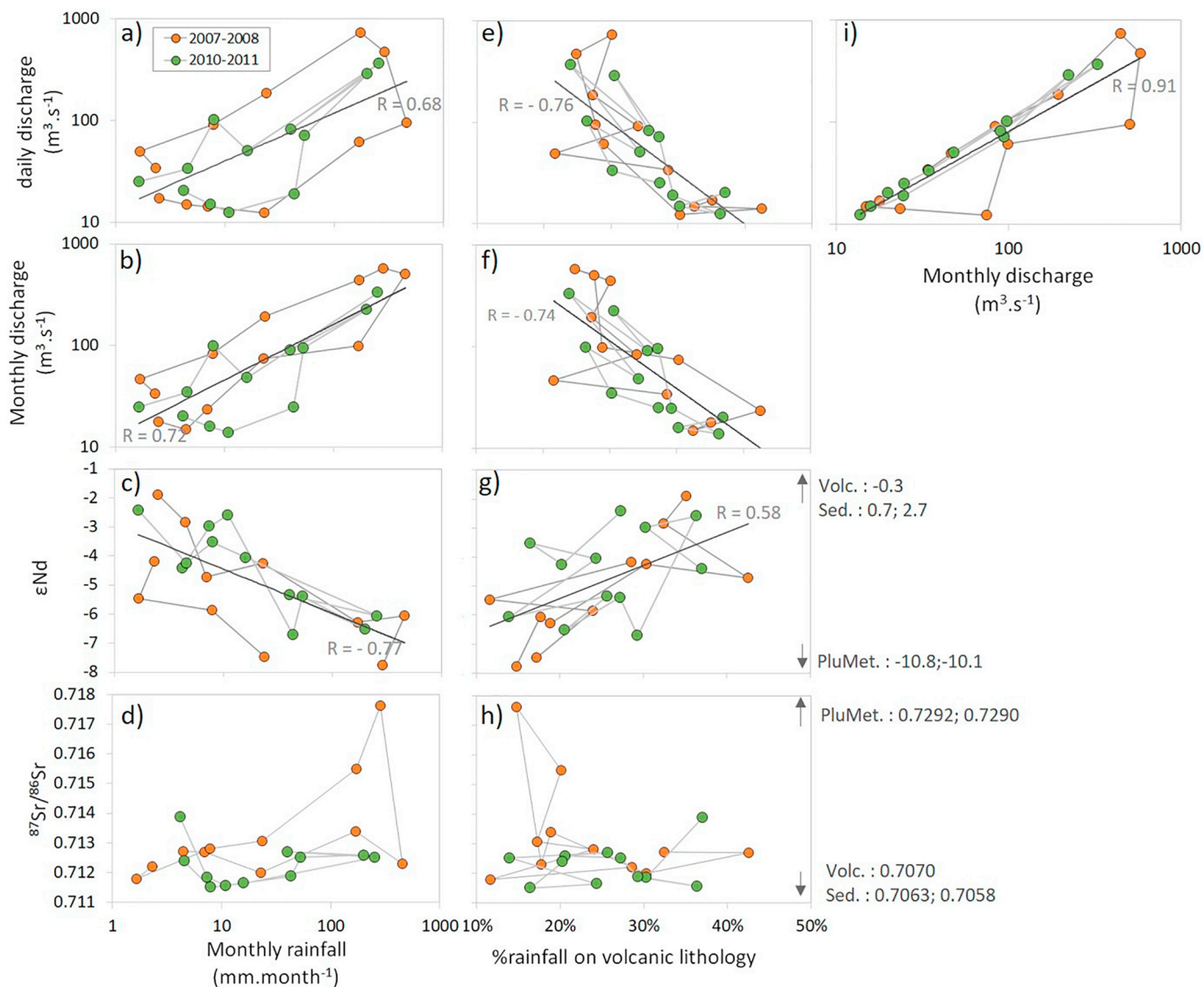


Fig. 8. a) daily discharge, b) monthly discharge, c) ϵNd and d) $^{87}Sr/^{86}Sr$ vs monthly rainfall. e) daily discharge, f) monthly discharge, g) ϵNd and h) $^{87}Sr/^{86}Sr$ vs proportion of rainfall received by the volcanic lithology (reported in Fig. 2). i) daily discharge vs monthly discharge. Only significant correlation coefficients (p -value < .01) are reported. They considered all points of both hydrological cycles. The abbreviation Volc, PluMet and Sed refers to the values determined for SPM samples from the volcanic, the plutonic/metamorphic and the sedimentary sub-basins, respectively (see Section 3 for details).

data along the Peruvian Pacific coast, Rau et al. (2017) highlighted that the main modes of influence of the ENSO increased rainfall over downstream regions in Northern Peru during extreme El Niño events and decreased rainfall over upstream regions along the Pacific slope during central Pacific El Niño events. Given the results presented in this study, we expect more radiogenic $^{87}Sr/^{86}Sr$ and more negative ϵNd values during strong El Niño events for SPM of the northern basins because of lower rainfall on volcanic rocks relative to downstream areas during these events. During the La Nina events, higher rainfall in the more elevated areas occupied by volcanic rocks (high ϵNd values) and low rainfall along the coast and downstream region would produce SPM with higher ϵNd values and less radiogenic Sr isotopic compositions (Fig. 9). As sediments fluxes depend on rainfall amount especially during exceptionally rainy years (Morera et al., 2017), a comparison of Sr and Nd isotopes with the sedimentation rate, can potentially indicate if a relation exists between rainfall locations and rainfall amount during the period covered by the core.

5. Conclusion

We investigated the geochemistry of the riverine SPM (Suspended

Particulate Matter) transported by the Tumbes River at a monthly frequency along two hydrological years, including a wet (2007–2008) and a normal (2010–2011) year. We also analyzed the SPM of 2 monolithological tributaries representative of the lithological diversity of the basin (i.e. volcanic and plutonic/metamorphic) and a sedimentary sub-basins located below a volcanic domain. This constructed geochemical database, never produced so far for an Andean River, is compared with the hydrology, climate and geology data available over the studied basin.

The clay mineralogy is almost homogenous with a CIA nearly constant along the hydrological year, showing that these two parameters are not adapted to track the SPM sources variability. However Sr and Nd isotopes signatures change during the hydrological year and they covariate with discharge, SPM concentration and SPM fluxes. The variability of ϵNd (from -7.8 to -1.9) along the two analyzed hydrological years is coherent with the spatial rainfall distribution throughout the basin. Less radiogenic values are measured during rainy season when the relative contribution of the upper part of the basin, dominated by volcanic rocks (a more radiogenic endmember), is lower. Therefore, Nd isotope composition constitutes a direct proxy of rainfall spatial distribution, which is related to SPM and water fluxes along the

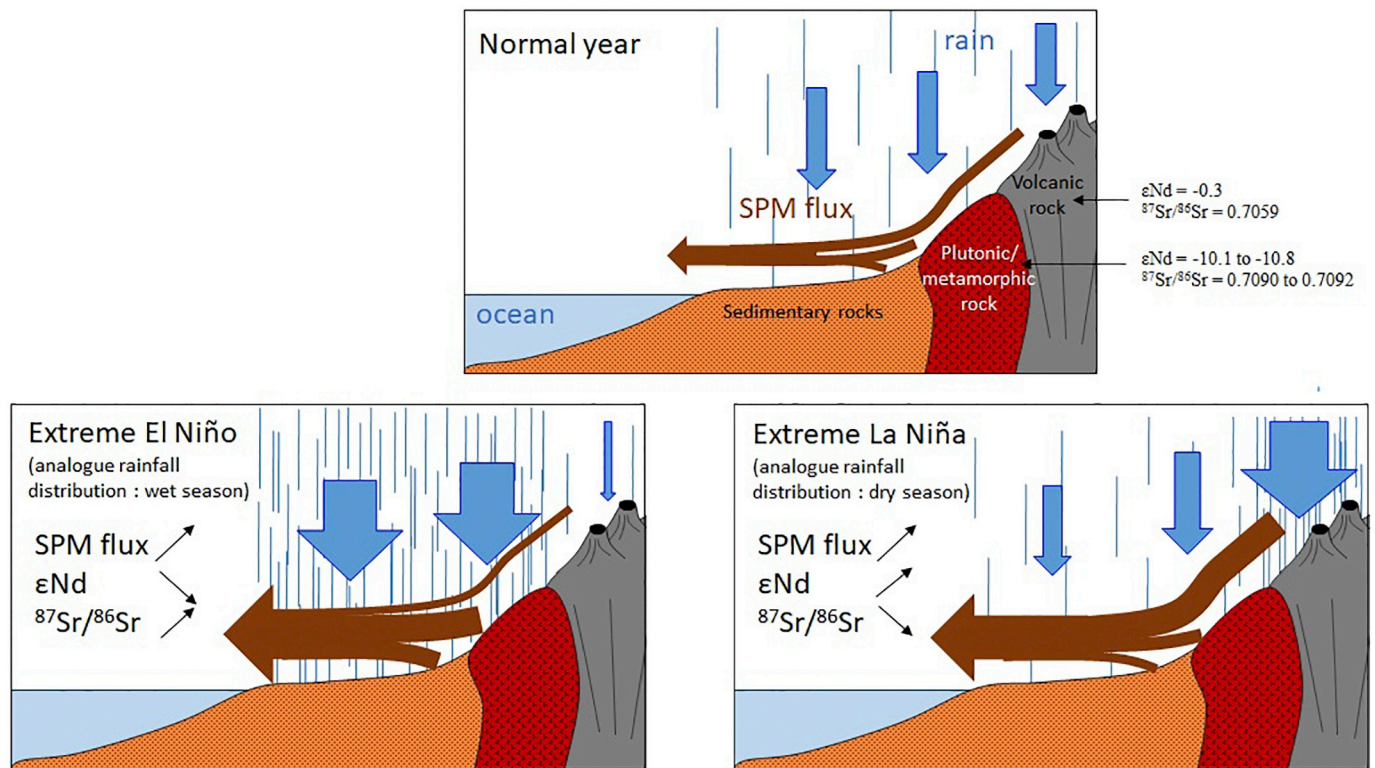


Fig. 9. Schematic representation of the main SPM flux and their Nd and Sr isotope signature in response to the extreme ENSO modes.

hydrological year. With the exception of two samples, Sr isotope composition is less variable along the studied periods ($^{87}\text{Sr}/^{86}\text{Sr} = 0.7115$ to 0.7139) as this isotope ratio traces only exceptionally high hydrological conditions during exceptional high rainfall/discharge years. The two exceptions of higher radiogenic Sr ($^{87}\text{Sr}/^{86}\text{Sr} = 0.7176$ and 0.7155) were measured during abnormal hydrological conditions of March and April 2008 and can be most likely attributed to higher contributions of the plutonic/metamorphic lithological domain. Interestingly, these geochemical tracers are highly linked to hydrological and erosional processes of the Tumbes basin.

These isotopic tracers are powerful proxies that can be used to reconstruct paleoclimate based on either sediment cores from floodplains and/or continental margin basins as well as to identify the main processes of seasonal SPM mobilization in the Tumbes basin. Moreover, these tracers allow us to detect changes in rainfall and hydrological regimes both in terms of water fluxes and rainfall distribution at the scale of the Tumbes River, which is a basin highly sensitive to the diversity of ENSO events. Interestingly, the geology mapped along the whole Pacific coast in Ecuador and Peru corresponds to the same geological distribution. Therefore, the results of the present study can be generalized for these contexts and potentially allows reconstructing paleo ENSO variabilities and other climate modes affecting the Pacific coast climate from decadal to multi-millennial timescales.

Supplementary data to this article can be found online at <https://doi.org/10.1016/j.gloplacha.2019.103080>.

Acknowledgments

This study was supported by the Peruvian Ministerio de Economía y Finanzas PPR-068 program “Reducción de Vulnerabilidad y Atención de Emergencias por Desastres”, INNOVATE PERÚ (www.innovateperu.gob.pe) and FONDECYT through the projects “Monitoreo, caracterización identificación de las principales fuentes de erosión y sedimentos durante fuertes crecidas o eventos extremos El Niño en las cuencas binacionales Puyango-Tumbes y Zarumilla” and “Monitoreo de Sedimentos Ante Riesgos y Desastres (MoSARD)”, respectively. This work was also funded by the French Institut de Recherche pour le

Développement (IRD) and the French Institut des Sciences de l'Univers (INSU) through the HYBAM Observatory which is part of the Research Infrastructure OZCAR (French network of Critical Zone Observatories: Research and Applications), by French Agence nationale de la recherche (ANR) ANR-15-JCLI-0003-03 BELMONT FORUM PACMEDY and by the Programme “Emergences” of the City of Paris “Chemical weathering of sediments in large tropical floodplains” (agreement 205DDEEES165). We especially thank Pascal Fraizy, Philippe Vauchel, William Santini, Elisa Armijos, Nore Arevalo, the SENAMHI (Servicio Nacional de Meteorología e Hidrología — Lima Peru and La Paz Bolivia), the UNALM (Universidad Nacional Agraria de La Molina, Lima — Peru) and all members of the SO HYBAM (Hydrogeodynamics of the Amazon basin), for providing hydrological and SPM sampling and concentration data. We also thank Mathieu Benoit for his help in TIMS analyses, Michel Thibaut for the DRX analyses both from the GET Laboratory and Sandrine Caquineau from the LOCEAN laboratory for her help in semi-quantitative analyses on DRX data. We also thank Nicole Fernandez for the English proofreading of this manuscript. We also thank Jamie Woodward (University of Manchester) and an anonymous reviewer for their constructive comments along the review process.

References

- Allègre, C.J., Dupré, B., Négrel, P., Gaillardet, J., 1996. Sr Nd Pb isotope systematics in Amazon and Congo River systems: constraints about erosion processes. *Chemical Geology* 131, 93–112. [https://doi.org/10.1016/0009-2541\(96\)00028-9](https://doi.org/10.1016/0009-2541(96)00028-9).
- Ancellin, M.-A., Samaniego, P., Vlastélic, I., Nauret, F., Gannoun, A., Hidalgo, S., 2017. Arc-arc versus along-arc Sr-Nd-Pb isotope variations in the Ecuadorian volcanic arc. *Geochim. Geophys. Geosyst.* 18, 1163–1188. <https://doi.org/10.1002/2016GC006679>.
- Armijos, E., Laraque, A., Barba, S., Bourrel, L., Ceron, C., Lagane, C., Magat, P., Moquet, J.S., Pombosa, R., Sondag, F., Vera, A., Guyot, J.L., 2013. Yields of suspended sediment and dissolved solids from the Andean basins of Ecuador. *Hydro. Sci. J.* 58, 1478–1494.
- Bayon, G., Toucanne, S., Skonieczny, C., André, L., Bermell, S., Cheron, S., Dennielou, B., Etoubleau, J., Freslon, N., Gauchery, T., Germain, Y., Jorry, S.J., Ménot, G., Monin, L., Ponzevera, E., Rouget, M.-L., Tachikawa, K., Barrat, J.A., 2015. Rare earth elements and neodymium isotopes in world river sediments revisited. *Geochim. Cosmochim. Acta* 170, 17–38. <https://doi.org/10.1016/j.gca.2015.08.001>.
- Bendix, J., Trachte, K., Palacios, E., Rollenbeck, R., Göttlicher, D., Nauss, T., Bendix, A., 2011. El Niño meets La Niña—Anomalous rainfall patterns in the “traditional” El Niño region of southern Ecuador. *Erdkunde* 65, 151–167.

- Bird, B.W., Abbott, M.B., Vuille, M., Rodbell, D.T., Stansell, N.D., Rosenmeier, M.F., 2011. A 2,300-year-long annually resolved record of the south American summer monsoon from the Peruvian Andes. *Proc. Natl. Acad. Sci.* 108 (21), 8583. <https://doi.org/10.1073/pnas.1003719108>.
- Biscaye, P.E., 1965. Mineralogy and Sedimentation of recent Deep-Sea Clay in the Atlantic Ocean and Adjacent Seas and Oceans. *GSA Bull.* 76, 803–832. [https://doi.org/10.1130/0016-7606\(1965\)76\[803:MASORD\]2.0.CO;2](https://doi.org/10.1130/0016-7606(1965)76[803:MASORD]2.0.CO;2).
- Blum, J.D., Erel, Y., 2003. 5.12 - Radiogenic isotopes in weathering and hydrology. In: Holland, H.D., Turekian, K.K. (Eds.), *Treatise on Geochemistry*. Pergamon, Oxford, pp. 365–392.
- Bouchez, J., Gaillardet, J., France-Lanord, C., Maurice, L., Dutra-Maia, P., 2011. Grain size control of river suspended sediment geochemistry: clues from Amazon River depth profiles. *Geochem. Geophys. Geosyst.* 12.
- Bustamante Rosell, M.G., Cruz, F.W., Sifeddine, A., Cheng, H., Apaestegui, J., Vuille, M., Strikis, N., Moquet, J.S., Novello, V., Guyot, J.L., Edwards, R.L., 2016. Holocene changes in monsoon precipitation in the Andes of NE Peru based on $\delta^{18}O$ speleothem records. *Quat. Sci. Rev.* 146, 274–287. <https://doi.org/10.1016/j.quascirev.2016.05.023>.
- Capotondi, A., Wittenberg, A.T., Newman, M., Di Lorenzo, E., Yu, J.Y., Braconnot, P., Cole, J., Dewitte, B., Giese, B., Guilyardi, E., Jin, F.F., 2015. Understanding ENSO diversity. *Bull. Am. Meteorol. Soc.* 96 (6), 921–938.
- Carré, M., Azzoug, M., Bentaleb, I., Chase, B.M., Fontugne, M., Jackson, D., Ledru, M.-P., Maldonado, A., Sachs, J.P., Schauer, A.J., 2012. Mid-Holocene mean climate in the south eastern Pacific and its influence on South America. *Quat. Int.* 253, 55–66. <https://doi.org/10.1016/j.quaint.2011.02.004>.
- Chauvel, C., Blichert-Toft, J., 2001. A hafnium isotope and trace element perspective on melting of the depleted mantle. *Earth Planet. Sci. Lett.* 190, 137–151. [https://doi.org/10.1016/S0012-821X\(01\)00379-X](https://doi.org/10.1016/S0012-821X(01)00379-X).
- Ehler, C., Grasse, P., Frank, M., 2013. Changes in silicate utilisation and upwelling intensity off Peru since the last Glacial Maximum – insights from silicon and neodymium isotopes. *Quat. Sci. Rev.* 72, 18–35. <https://doi.org/10.1016/j.quascirev.2013.04.013>.
- Espinoza, J.C., Ronchail, J., Guyot, J.L., Junquas, C., Drapeau, G., Martinez, J.M., Santini, W., Vauchel, P., Lavado, W., Ordoñez, J., Espinoza, R., 2012. From drought to flooding: understanding the abrupt 2010–11 hydrological annual cycle in the Amazonas river and tributaries. *Environ. Res. Lett.* 7, 24008. <https://doi.org/10.1088/1748-9326/7/2/024008>.
- Faure, G., Mensing, T.M., 2004. *Isotopes. Principles and Applications*, 3rd edition. John Wiley and Sons Ltd. ed.
- Goldstein, S.L., Hemming, S.R., 2003. 6.17 - Long-lived Isotopic tracers in oceanography, paleoceanography, and Ice-sheet Dynamics. In: Holland, H.D., Turekian, K.K. (Eds.), *Treatise on Geochemistry*. Pergamon, Oxford, pp. 453–489.
- Guyot, J.L., Jouanneau, J.M., Soares, L., Boaventura, G.R., Maillet, N., Lagane, C., 2007. Clay mineral composition of river sediments in the Amazon Basin. *CATENA* 71, 340–356.
- Hodell, D.A., Kamenov, G.D., Hathorne, E.C., Zachos, J.C., Röhl, U., Westerhold, T., 2007. Variations in the strontium isotope composition of seawater during the Paleocene and early Eocene from ODP Leg 208 (Walvis Ridge). *Geochemistry, Geophysics, Geosystems* 8. <https://doi.org/10.1029/2007GC001607>.
- Höppner, N., Lucassen, F., Chiessi, C.M., Sawakuchi, A.O., Kasemann, S.A., 2018. Holocene provenance shift of suspended particulate matter in the Amazon River basin. *Quat. Sci. Rev.* 190, 66–80. <https://doi.org/10.1016/j.quascirev.2018.04.021>.
- Huaman, L., Takahashi, K., 2016. The vertical structure of the eastern Pacific ITCZs and associated circulation using the TRMM Precipitation Radar and in situ data. *Geophys. Res. Lett.* 43, 8230–8239. <https://doi.org/10.1002/2016GL068835>.
- Jacobsen, S.B., Wasserburg, G.J., 1980. Sm-Nd isotopic evolution of chondrites. *Earth Planet. Sci. Lett.* 50, 139–155. [https://doi.org/10.1016/0012-821X\(80\)90125-9](https://doi.org/10.1016/0012-821X(80)90125-9).
- Krom, M.D., Stanley, J.D., Cliff, R.A., Woodward, J.C., 2002. Nile river sediment fluctuations over the past 7000 yr and their key role in sapropel development. *Geology* 30, 71–74.
- Lagos, P., Silva, Y., Nickl, E., Mosquera, K., 2008. El Niño – related precipitation variability in Perú. *ADGEO* 14, 231–237. <https://doi.org/10.5194/adgeo-14-231-2008>.
- Lavado Casimiro, W.S., Ronchail, J., Labat, D., Espinoza Villar, J.-C., Guyot, J.L., 2012. Basin-scale analysis of rainfall and runoff in Peru (1969–2004): Pacific, Titicaca and Amazonas drainages. *Hydrol. Sci. J.* 57, 1–18.
- Lavado, W., Espinoza, J.C., 2014. Impactos de El Niño y La Niña en las lluvias del Perú. *Rev. Brasil. Meteorol.* 29, 171–182.
- Lavado, W., Fernandez, C., Vega, F., Caycho, T., Endara, S., Huerta, A., Obando OF, 2016. PISCO: peruvian interpolated data of the SENAMHI's climatological and hydrological observations. *Precipitación v1.0*. Serv. Nacional Meteorol. Hidrol. 1–4.
- Li, T., Xu, Z., Lim, D., Chang, F., Wan, S., Jung, H., Choi, J., 2015. Sr–Nd isotopic constraints on detrital sediment provenance and paleoenvironmental change in the northern Okinawa Trough during the late Quaternary. *Palaeogeogr. Palaeoclimatol. Palaeoecol.* 430, 74–84. <https://doi.org/10.1016/j.palaeo.2015.04.017>.
- Liu, Z., Zhao, Y., Colin, C., Statterger, K., Wiesner, M.G., Huh, C.-A., Zhang, Y., Li, X., Sompongchaiyakul, P., You, C.-F., Huang, C.-Y., Liu, J.T., Siringan, F.P., Le, K.P., Sathiamurthy, E., Hantoro, W.S., Liu, J., Tuo, S., Zhao, S., Zhou, S., He, Z., Wang, Y., Bunsomboonsakul, S., Li, Y., 2016. Source-to-sink transport processes of fluvial sediments in the South China Sea. *Earth Sci. Rev.* 153, 238–273. <https://doi.org/10.1016/j.earscirev.2015.08.005>.
- Lugmair, G.W., Shimamura, T., Lewis, R.S., Anders, E., 1983. Samarium-146 in the early Solar System: evidence from Neodymium in the Allende Meteorite. *Science* 222 (4627), 1015–1018.
- Mao, C., Chen, J., Yuan, X., Yang, Z., Ji, J., 2011. Seasonal variations in the Sr–Nd isotopic compositions of suspended particulate matter in the lower Changjiang River: Provenance and erosion constraints. *Chin. Sci. Bull.* 56, 2371–2378. <https://doi.org/10.1007/s11434-011-4589-6>.
- Marshall, B.G., Veiga, M.M., Kaplan, R.J., Adler Miserendino, R., Schudel, G., Bergquist, B.A., Guimarães, J.R.D., Sobral, L.G.S., Gonzalez-Mueller, C., 2018. Evidence of trans-boundary mercury and other pollutants in the Puyango-Tumbes River basin, Ecuador–Peru. *Environ. Sci.* 20, 632–641. <https://doi.org/10.1039/C7EM00504K>.
- McLennan, S.M., Hemming, S., McDaniel, D.K., Hanson, G.N., 1993. *Geochemical approaches to sedimentation, provenance, and tectonics*. In: Johnson, M.J., Basu, A. (Eds.), *Processes Controlling the Composition of Clastic Sediments*. Geological Society of America.
- Moatar, F., Meybeck, M., Raymond, S., Birgand, F., Curie, F., 2013. River flux uncertainties predicted by hydrologic variability and riverine material behaviour. *Hydrol. Process.* 27, 3535–3546.
- Moquet, J.-S., Crave, A., Viers, J., Seyler, P., Armijos, E., Bourrel, L., Chavarri, E., Lagane, C., Laraque, A., Lavado Casimiro, W.S., Pombosa, R., Noriega, L., Vera, A., Guyot, J.-L., 2011. Chemical weathering and atmospheric/soil CO₂ uptake in the Andean and Foreland Amazon basins. *Chem. Geol.* 287, 1–26. <https://doi.org/10.1016/j.chemgeo.2011.01.005>.
- Moquet, J.S., Viers, J., Crave, A., Armijos, E., Lagane, C., Lavado, W., Pepin, E., Pombosa, R., Noriega, L., Santini, W., Guyot, J.L., 2014. Comparison between silicate weathering and physical erosion rates in Andean basins of Amazon river. *Procedia Earth Plan. Sci.* 10, 275–279. <https://doi.org/10.1016/j.proeps.2014.08.061>.
- Moquet, J.-S., Guyot, J.-L., Morera, S., Crave, A., Rau, P., Vauchel, P., Lagane, C., Sondag, F., Lavado, C.W., Pombosa, R., Martinez, J.-M., 2018. Temporal variability and annual budget of inorganic dissolved matter in Andean Pacific Rivers located along a climate gradient from northern Ecuador to southern Peru. *Compt. Rendus Geosci.* 350, 76–87. <https://doi.org/10.1016/j.crte.2017.11.002>.
- Morera, S.B., Condom, T., Crave, A., Steer, P., Guyot, J.L., 2017. The impact of extreme El Niño events on modern sediment transport along the western Peruvian Andes (1968–2012). *Sci. Rep.* 7, 11947. <https://doi.org/10.1038/s41598-017-12220-x>.
- Pin, C., Briot, D., Bassin, C., Poitras, F., 1994. Concomitant separation of strontium and samarium-neodymium for isotopic analysis in silicate samples, based on specific extraction chromatography. *Anal. Chim. Acta* 298, 209–217. [https://doi.org/10.1016/0003-2670\(94\)00274-6](https://doi.org/10.1016/0003-2670(94)00274-6).
- Rau, P., Bourrel, L., Labat, D., Melo, P., Dewitte, B., Frappart, F., Lavado, W., Felipe, O., 2017. Regionalization of rainfall over the Peruvian Pacific slope and coast. *Int. J. Climatol.* 37, 143–158. <https://doi.org/10.1002/joc.4693>.
- Roddaz, M., Viers, J., Brusset, S., Baby, P., Hérail, G., 2005. Sediment provenances and drainage evolution of the Neogene Amazonian foreland basin. *Earth Planet. Sci. Lett.* 239, 57–78.
- Roddaz, M., Viers, J., Moreira-Turcq, P., Blondel, C., Sondag, F., Guyot, J.-L., Moreira, L., 2014. Evidence for the control of the geochemistry of Amazonian floodplain sediments by stratification of suspended sediments in the Amazon. *Chem. Geol.* 387, 101–110.
- Rousseau, T.C.C., Roddaz, M., Moquet, J.-S., Handt Delgado, H., Calves, G., Bayon, G., 2019. Controls on the geochemistry of suspended sediments from large tropical South American rivers (Amazon, Orinoco and Maroni). *Chem. Geol.* 522, 38–54. <https://doi.org/10.1016/j.chemgeo.2019.05.027>.
- Scott, E.M., Allen, M.B., Macpherson, C.G., McCaffrey, K.J.W., Davidson, J.P., Saville, C., Ducea, M.N., 2018. Andean surface uplift constrained by radiogenic isotopes of arc lavas. *Nat. Commun.* 9, 969. <https://doi.org/10.1038/s41467-018-03173-4>.
- Segura, H., Junquas, C., Espinoza, J.C., Vuille, M., Jauregui, Y.R., Rabatel, A., Condom, T., Lebel, T., 2019. New insights into the rainfall variability in the tropical Andes on seasonal and interannual time scales. *Clim. Dyn.* <https://doi.org/10.1007/s00382-018-4590-8>.
- Singh, S.K., Rai, S.K., Krishnaswami, S., 2008. Sr and Nd isotopes in river sediments from the Ganga Basin: Sediment provenance and spatial variability in physical erosion. *J. Geophys. Res.* 113. <https://doi.org/10.1029/2007JF009099>.
- Sulca, J., Takahashi, K., Espinoza, J.C., Vuille, M., Lavado-Casimiro, W., 2018. Impacts of different ENSO flavors and tropical Pacific convection variability (ITCZ, SPCZ) on austral summer rainfall in South America, with a focus on Peru. *Int. J. Climatol.* 38 (1), 420–435. <https://doi.org/10.1002/joc.5185>.
- Takahashi, K., Martínez, A., 2017. The very strong coastal El Niño in 1925 in the far-eastern Pacific. *Clim. Dyn.* <https://doi.org/10.1007/s00382-017-3702-1>.
- Thompson, L.G., Mosley-Thompson, E., Davis, M.E., Zagorodnov, V.S., Howat, I.M., Mikhailenko, V.N., Lin, P.-N., 2013. Annually Resolved Ice Core Records of Tropical Climate Variability over the Past ~1800 Years. 340. pp. 945–950.
- van der Lubbe, H.J.L., Frank, M., Tjallingii, R., Schneider, R.R., 2016. Neodymium isotope constraints on provenance, dispersal, and climate-driven supply of Zambesi sediments along the Mozambique margin during the past ~45,000 years. *Geochem. Geophys. Geosyst.* 17, 181–198. <https://doi.org/10.1002/2015GC006080>.
- Vauchel, P., 2005. HYDRACCESS : Software for Management and Processing of Hydro - Meteorological Data. www.mpl.ird.fr/hybam/outils/hydraccess.
- Viers, J., Roddaz, M., Filizola, N., Guyot, J.-L., Sondag, F., Brunet, P., Zouiten, C., Boucayrand, C., Martin, F., Boaventura, G.R., 2008. Seasonal and provenance controls on Nd–Sr isotopic compositions of Amazon rivers suspended sediments and implications for Nd and Sr fluxes exported to the Atlantic Ocean. *Earth Planet. Sci. Lett.* 274.
- Wara, M.W., Ravelo, A.C., Delaney, M.L., 2005. Permanent El Niño-like conditions during the Pliocene warm period. *Science* 309, 758. <https://doi.org/10.1126/science.1112596>.
- Woodward, J., Macklin, M., Fielding, L., Millar, I., Spencer, N., Welsby, D., Williams, M., 2015. Shifting sediment sources in the world's longest river: a strontium isotope record for the Holocene Nile. *Quat. Sci. Rev.* 130, 124–140. <https://doi.org/10.1016/j.quascirev.2015.10.040>.